Enhancements in Conductivity and Thermal and Conductive Stabilities of Electropolymerized Polypyrrole with Caprolactam-Modified Clay

Yu-Chuan Liu* and Chenh-Jung Tsai

Department of Chemical Engineering, Van Nung Institute of Technology, 1, Van Nung Road, Shuei-Wei Li, Chung-Li City, Taiwan, Republic of China

Received August 1, 2002. Revised Manuscript Received October 30, 2002

In this study, a polypyrrole (PPy)/caprolactam-modified montmorillonite (MMT) clay composite was electropolymerized on a gold substrate. Basically, the nucleation and growth were instantaneous three-dimensional processes before and after nuclei overlapping for both pure PPy and the composite electropolymerizations. However, a distinguishable feature can be observed. The surface morphology of the resulting composite is denser and more compact. The composite demonstrates an extremely high oxidation level and oxidation degree of 0.41 and 0.59 revealed from the analyses of X-ray photoelectron spectroscopy (XPS) and surface-enhanced Raman scattering (SERS), respectively. The thermal stability of PPy is improved, as shown from thermogravimetric analysis (TGA), due to the modification of the incorporated clay. Also, the conductivity of the composite was significantly increased (∼12 times) and aging is depressed compared to that of pure PPy.

Introduction

Among a number of conducting polymers (CP), polypyrrole (PPy), has attracted considerable attention because it offers reasonably high conductivity and has fairly good environmental stability, and it can be widely used in batteries,[1,2] supercapacitors,[3] sensors,[4,5] anhydrous electrorheological fluids,[6] microwave shielding, and corrosion protection.[7,8] As we know, the electrical conductivity of PPy is attributed to the electrons hopping along and across the polymer chains with conjugating bonds.[9,10] As a result, more positively charged PPy, more electron holes available, longer polymer chains, and more coplanarity between interchains are favorable for a higher conductivity performance. The conductivity of oxidized PPy can be increased to a level of 10^3 S cm^{-1}, or higher, depending on the method of preparation and the doped ion.[11−13] However, the potential uses are often diminished due to its sensitivity to oxygen or poor mechanical properties.

To achieve a new function of PPy, one of the most efficient means is to prepare PPy-based composite films into which new chemical components, such as nanoparticles of metal oxides[14,15] and metals,[16−18] are introduced. On the other hand, clay minerals, especially montmorillonite (MMT), have recently been adapted to the field of nanocomposites because of their small particle sizes and intercalation properties.[19−21] MMT, a hydrous alumina silicate mineral whose lamellae are constructed from an octahedral alumina sheet sandwiched between two tetrahedral silica sheets, exhibits a net negative charge on the lamellar surface and causes adsorption of cations, such as Na^+ or Ca^{2+}. The cationic character acting over a very large interlamellar surface enables physical and chemical interactions with monomers which are subsequently polymerized, or with polymers containing appropriate functionalities.[20] As shown in the literature, most of the CP/clay composites, such as PPy-based[22,23] and polyaniline-based[24] clays

* To whom all correspondence should be addressed. Tel: 886-3-4515811 ext 540. Fax: 886-2-86638557. E-mail: liuyc@cc.vit.edu.tw.

(1) Kim, J. U.; Jeong, I. S.; Moon, S. I.; Gu, H. B. *J. Power Sources* **2001**, *97*, 450.
(2) Chen, J. H.; Huang, Z. P.; Wang, D. Z.; Yang, S. X.; Li, W. Z.; Wen, J. G.; Ren, Z. F. *Synth. Met.* **2001**, *125*, 289.
(3) Jurewicz, K.; Delpeux, S.; Bertagna, V.; Beguin, F.; Frackowiak, E. *Chem. Phys. Lett.* **2001**, *347*, 36.
(4) Lin, C. W.; Hwang, B. J.; Lee, C. R. *Mater. Chem. Phys.* **1998**, *55*, 139.
(5) Hepel, M. *J. Electrochem. Soc.* **1998**, *145*, 124.
(6) Goodwin, J. W.; Markham, G. M.; Vinent, B. *J. Phys. Chem. B* **1997**, *101*, 1961.
(7) Truong, V. T.; Lai, P. K.; Moore, B. T.; Muscat, R. F.; Russo, M. S. *Synth. Met.* **2000**, *110*, 1.
(8) Buckley, L. J.; Eashov, M. *Synth. Met.* **1996**, *78*, 1.
(9) Scrosati, B. *Application of Electroactive Polymers*, 1st ed.; Chapman & Hall: London, 1993; Chapter 2, p 33.
(10) Erlandsson, R.; Inganas, O.; Lundstron, I.; Salaneck, W. R. *Synth. Met.* **1985**, *10*, 303.
(11) Samuelson, L. A.; Druy, M. A. *Macromolecules* **1986**, *19*, 824.
(12) Patil, A.; Ikenone, Y.; Wundl, F.; Heeger, A. *J. Am. Chem. Soc.* **1987**, *109*, 1858.
(13) Allen, N. S.; Murray, K. S.; Fleming, R. J.; Saunders, B. R.; *Synth. Met.* **1997**, *87*, 237.
(14) Zhang, P.; Yang, Z. H.; Wang, D. J.; Kan, S.H.; Chai, X. D.; Liu, J. Z.; Li, T. J. *Synth. Met.* **1997**, *84*, 165.
(15) Cong, H. Nguyen; Abbassi, K. E.; Chartier, P. *Electrochem. Solid State Lett.* **2000**, *3*, 192.
(16) Cioffi, N.; Torsi, L.; Sabbatini, L.; Zambonin, P. G.; Zacheo, T. B. *J. Electroanal. Chem.* **2000**, *488*, 42.
(17) Cioffi, N.; Torsi, L.; Losito, I.; Sabbatini, L.; Zambonin, P. G.; Zacheo, T. B. *Electrochim. Acta* **2001**, *46*, 4205.
(18) Kim, H.; Chang, W. *Synth. Met.* **1999**, *101*, 150.
(19) Biswas, M.; Ray, S. S. *Polymer* **1998**, *39*, 6423.
(20) Kim, J. W.; Kim, S. G.; Choi, H. J.; Jhon, M. S. *Macromol. Rapid Commun.* **1999**, *20*, 450.
(21) Kim, B. H.; Jung, J. H.; Kim, J. W.; Choi, H. J.; Joo, J. *Synth. Met.* **2001**, *117*, 115.
(22) Ramachandran, K.; Lerner, M. M. *J. Electrochem. Soc.* **1997**, *144*, 3739.
(23) Ray, S. S.; Biswas, M. *Mater. Res. Bull.* **1999**, *34*, 1187.

10.1021/cm020194c CCC: $25.00
Published on Web 12/11/2002

composites, were chemically synthesized. The formation of the nanocomposites due to the intercalation was confirmed via transmission electron micrograph (TEM) or X-ray diffraction (XRD) analyses. Faguy et al.[25] reported that a PPy/clay composite was successfully synthesized as the ferric sites present at the accessible surfaces of the clay particles chemically oxidized the aromatic heterocycle. Ramachandran and Lerner[22] reported that a chemically prepared PPy/clay nanocomposite exhibits redox chemistry at potentials ($V_{p,c}$ = −1500, $V_{p,a}$ = −1100 mV) approximately 1 V more negative than those in native PPy. Ray and Biswas[23] reported that PPy/clay nanocomposites can be prepared through the polymerization of pyrrole with clay and $FeCl_3$-impregnated clay. The XRD analyses revealed no change in d_{001} spacing in clay, suggesting no intercalation into the clay lamellae. Cho et al.[26] reported that surfactant bilayers adsorbed on a silicon−titanium zeolite can be used as templates to produce colloidal nanocomposites with a PPy shell which exhibit good colloidal stability and an enhanced conductivity.

It is also known that the nucleation and growth mechanisms of conducting polymers are very similar to those of metals.[27,28] Thus the mechanism for conducting polymer growth can be proved using the theory model of metal growth.[29,30] As shown in the literature,[22,23,25,26] most of the PPy/clay nanocomposites were prepared by chemical methods. However, PPy films synthesized by electrochemical polymerization have the advantages of free-standing films available, higher conductivities, and better stabilities in air.[31,32] Also, other characteristics of electrochemically synthesized PPy/clay composites are worthy of further examination. To extend the applications of PPy in the fields of gas sensors, capacitors, and so on, the aim of this work is to electrochemically prepare a PPy/caprolactam-modified MMT clay composite. The caprolactam-modified MMT comes from the cationic exchange of caprolactam with Na^+ of the Na^+-MMT. Its interlayer spacing can enlarge from 7.2 to 14.9 Å to be facilely penetrated by a monomer. The effects on enhancements in conductivity, and thermal and conductivity stabilities for PPy are investigated. Also, the differences in nucleation and growth mechanisms between pure PPy and the PPy/clay composite are discussed.

Experimental Section

Preparation of PPy/Clay Composite Films. All the electrochemical experiments were performed in a three-compartment cell at room temperature (24 °C,) and were controlled by a potentiostat (model PGSTAT30, Eco Chemie). A sheet of gold, a 2 × 2 cm platinum sheet, and a Ag/AgCl were employed as the working, counter, and reference electrodes, respectively. The charges used in depositing PPy-based films were 5000 mC cm^{-2} for all of the experiments, except 100 mC cm^{-2} was used for the surface-enhanced Raman scattering (SERS) spectroscopy.[33]

Before electropolymerization, the gold electrode (model Minimet 1000, Buehler) was mechanically polished to a mirror finish with 1 and then 0.05 μm of alumina slurry. In a typical procedure, 1.6 g dm^{-3} caprolactam ($C_6H_{11}NO$)-modified MMT clay with interlayer spacing of 14.9 Å (purchased from Paikong Ceramic, Taiwan) was added in deionized water at pH = 7 and sonicated for 1 h. No precipitation was observed due to the electrostatic repulsive forces between the clay powders because the pH of the zero charge of the particles is 5.6.[26] Subsequently, 0.1 M $LiClO_4$ and 0.1 M pyrrole (C_4H_5N), which was doubly distilled under a reduced pressure, were dissolved with vigorous magnetic stirring in this emulsion solution for 30 min. During this step, the solution was deoxygenated with highly pure nitrogen. The pH of the electropolymerization bath was 6.8 higher than that of the zero charge of the clay, which is favorable for the preparation of the clay-modified PPy. Then the clay-modified PPy was electrochemically polymerized at 0.85 V versus Ag/AgCl in the clay-containing aqueous solution with slight magnetic stirring. For comparison, pure PPy was also polymerized with the same preparation condition as mentioned above but with no clay powders in the polymerization electrolyte. After each step the electrode was rinsed thoroughly with deionized water and then dried in a vacuum oven for 1 h. The samples were then placed in a sealed chamber with an oxygen-free atmosphere for further measurements.

Characteristics of PPy/Clay Composite Films. Before conductivity measurements the PPy-based films were stripped from the electrodes with clear adhesive tape. They had a mechanical stability that made them well suited for the measurements. The conductivities of PPy films were determined by using a four-probe technique with a direct current (dc) measurement at room temperature.[34] The surface morphology of PPy films was obtained using scanning electron microscopy (SEM, model S-4700, Hitachi). Thermogravimetric analysis (TGA) was performed using a Perkin-Elmer TGA7 at a heating rate of 15 °C/min under nitrogen. The orientations of PPy-based films were determined via XRD (model Dmax-B, Rigaku) analysis. The depth profile of Si (main element in clay) in the PPy/clay composite was measured via secondary ion mass spectroscopy (SIMS, model IMS-4f, Cameca) using cesium atoms as the primary ions. SERS spectra were obtained using a XY modular laser Raman spectrometer (Dior) employing a He−Ne laser of 1 mW radiating on the sample operating at 632.8 nm and a charge couple device (CCD) detector with 1 cm^{-1} resolution.

For the X-ray photoelectron spectroscopy (XPS) measurements a Physical Electronics PHI 1600 spectrometer with monochromatized Mg K_α radiation, 15 KV 250 W, and an energy resolution of 0.1−0.8% $\Delta E/E$ was used. To compensate for surface charging effects, all XPS spectra are referred to the C1s neutral carbon peak at 284.6 eV. The complex XPS and SERS peaks are deconvoluted into component Gaussian peaks using a peak separation and analysis software (PeakFit v4.0, AISN Software Inc.). In the XPS N 1s deconvolution, the four component peaks are located at ca. 398.0, 399.8, and at higher than 401 eV with equal value of half width at half-maximum (HWHM) of 2.0 eV to the utmost. In some situation, the peak position is prior to the equal HWHM. The aging test was performed in an atmosphere of 50% relative humidity (RH) and 20% volume concentration (v/v) of O_2 in the mixture of O_2 and N_2 at 30 °C for 60 days.

(24) Yeh, J. M.; Liou, S. J.; Lai, C. Y.; Wu, P. C.; Tsai, T. Y. *Chem. Mater.* **2001**, *13*, 1131.
(25) Faguy, P. W.; Lucas, R. A.; Ma, W. *Colloid Surface A* **1995**, *105*, 105.
(26) Cho, G.; Fung, B. M.; Glatzhofer, D. T.; Lee, J. S.; Shu, Y G. *Langmuir* **2001**, *17*, 456.
(27) Hwang, B. J.; Santhanam, R.; Lin, Y. L. *J. Electrochem. Soc.* **2000**, *147*, 2252.
(28) Hwang, B. J.; Santhanam, R.; Wu, C. R.; Tsai, Y. W. *Electroanalysis* **2001**, *13*, 37.
(29) Bard, K.; Tsakova, V.; Schultze, J. W. *Electrochim. Acta* **1992**, *37*, 2255.
(30) Dian, G.; Merlet, N.; Barbey, G.; Outurquin, F.; Paulmier, C. *J. Electroanal. Chem.* **1987**, *238*, 225.
(31) Balci, N.; Bayramli, E.; Toppare, L. *J. Appl. Polym. Sci.* **1997**, *64*, 667.
(32) Chen, X. B.; Devaux, J.; Issi, J. P.; Billaud, D. *Polym. Eng. Sci.* **1995**, *35*, 637.
(33) Liu, Y. C.; Hwang, B. J.; Jian, W. J. *Mater. Chem. Phys.* **2002**, *73*, 129.
(34) Liu, Y. C.; Hwang, B. J. *Thin Solid Films* **1999**, *339*, 233.

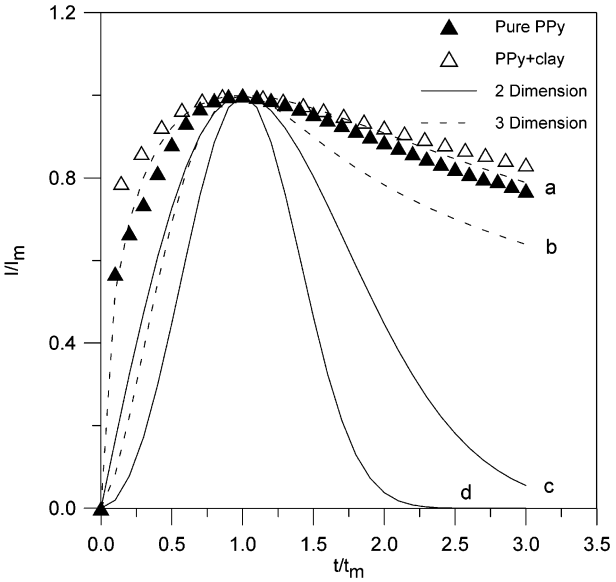

Figure 1. Dimensionless plots of $I-t$ curves for pyrrole polymerized on Au substrates in different electrolytes at 0.85 V vs Ag/AgCl, as compared with theoretical models for nucleation. Solid and hollow triangles represent pure PPy and the PPy/clay composite, respectively. Curves a and b represent 3D instantaneous and progressive models (dashed lines), respectively. Curves c and d represent 2D instantaneous and progressive models (solid lines), respectively.

Results and Discussion

Electropolymerization of Pyrrole with Clay. As shown in the literature,[27,35] there are two kinds of nucleation, namely instantaneous and progressive, and two types of growth, two-dimensional (2D) and three-dimensional (3D). The number of nuclei in the instantaneous nucleation mechanism is constant, and they grow on their former positions on the bare substrate surface without the formation of new nuclei. Hence, the radii of the nuclei are larger and the surface morphology is rougher. In progressive nucleation, the nuclei not only grow on their former positions on the bare substrate surface but also on new nuclei, which form smaller nuclei particles and the surface morphology is flatter. The current maximum (i_m) for the electropolymerization of pyrrole in different electrolytes obtained from the chronoamperometric curves are compared and fitted with the theoretical curves of 2D and 3D nucleation and growth obtained from those equations derived by Harrison and Thirsk[35] for current−time relation, as shown in Figure 1. It is clear that before and after nuclei overlapping (i_m), the experimental curves for both pure PPy and the PPy/clay composite are more or less consistent with the theoretical curve of the 3D instantaneous nucleation, but a positive deviation of i/i_m from the theoretical one is observed for the latter. Generally, the position of nucleation is favorably located on the defective surface, like edge or step on a surface, with a higher surface energy.[36] Before the electropolymerization of the PPy/clay composite, the surface of the Au substrate is markedly modified because the caprolactam-modified clay powders are easily adsorbed on the Au substrate in the emulsion solution. The pyrrole monomers are readily adsorbed in the positively charged lamellae and may be further polymerized into oligomers in the same manner as the polymerization of pyrrole with $FeCl_3$-impregnated clay.[23] Also, this emulsion system containing an aqueous medium can contribute to the maximization of the affinity between hydrophilic host (Au substrate) and hydrophobic guest (pyrrole monomer).[20] Thus, it results in more chance to nucleate and grow, and a correspondingly higher electropolymerization rate was observed for the PPy/clay composite.

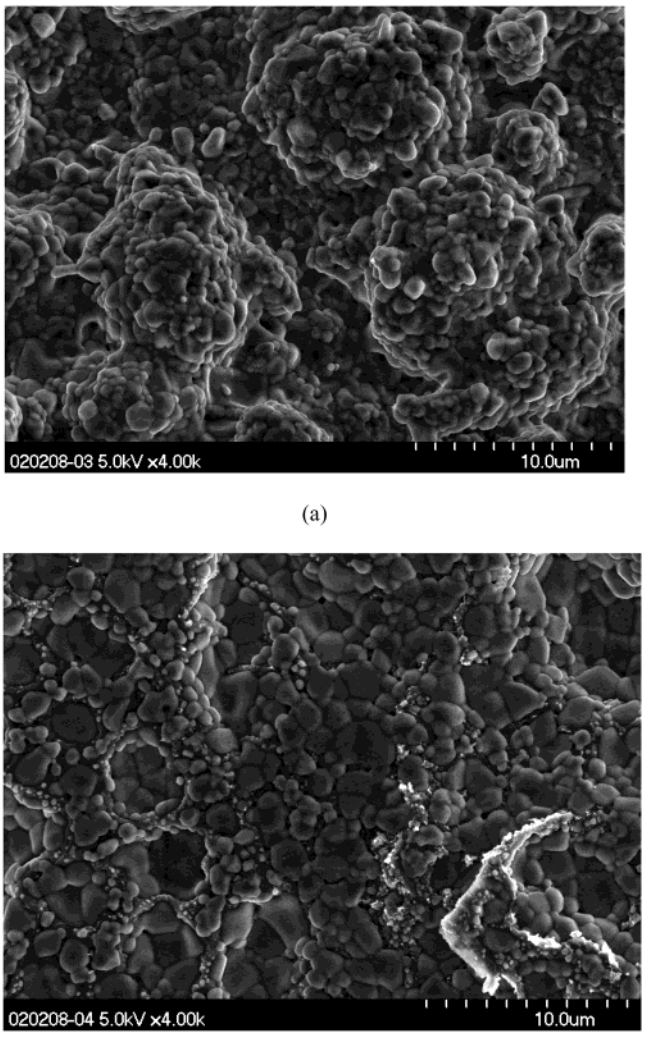

Figure 2. SEM micrographs of different PPy-based films: (a) pure PPy; (b) PPy/clay composite.

The SEM micrographs, as shown in Figure 2, reveal some interesting morphological differences between pure PPy and the PPy/clay composite. The film appears to be more densely packed for the PPy/clay composite. In contrast, pure PPy film shows a rougher and more porous surface morphology. As reported in the systems of PPy/Cu^+ complex,[37] PPy/PEO composite,[38] and unmodified PPy films,[39,40] denser and more compact

(35) Harrison, J. A.; Thirsk, H. R. *Electroanal. Chem*. Vol. 5, Marcel Dekker: New York, 1971; p 67.
(36) Hendvicks, S. A.; Kim, Y. T.; Bard, A. J. *J. Electrochem. Soc.* **1992**, *139*, 2818.
(37) Liu, Y. C.; Hwang, B. J. *J. Electroanal. Chem*. **2001**, *501*, 100.
(38) Liu, Y. C.; Hwang, B. J. *Thin Solid Films* **2000**, *360*, 1.
(39) Neoh, K.G.; Young, T. T.; Kang, E. T.; Tan, K. L. *J. Appl. Polym. Sci.* **1997**, *64*, 519.
(40) Dhanalakshmi, K.; Saraswathi, R.; Srinivasan, C. *Synth. Met.* **1996**, *82*, 237.

morphology would reflect on the enhancement of conductivity stability in the aging behavior of PPy films exposed to oxygen and water atmosphere. Moreover, an encouraging phenomenon is that the conductivity of PPy also can be enhanced, from 26.4 to 322 S cm^{-1}, by the formation of the PPy/clay composite. As shown in the literature,[41,42] the conductivity of the chemically synthesized nanocomposite of polyaniline intercalated into Na^+-MMT was decreased. This was attributed to the clay layer intercalated by a polyaniline layer inducing a weak interchain interaction between the polyaniline chains. Bhattacharya et al.[43] reported that PPy powders can be chemically polymerized in the presence of ultrafine ZrO_2 particles which act as a dispersant for pyrrole. The PPy powders were subsequent compressed by pelletization to measure the conductivity. The result indicated that the conductivity increases due to the improved coupling strength between the grains. In this work, the main reason accounting for enhancing the conductivity is likely that the PPy film is formed on the surface of the clay powders which act as a nucleus. This resulting composite becomes more compact, thus, it is contributive to electron hopping across the molecular interchains. As to the alternative, contribution to electron hopping along the polymer chains will be confirmed later from the XPS and SERS analyses.

Characteristics of the PPy/Clay Composite. The elemental depth profiles of pure PPy and the PPy/clay composite demonstrated in Figure 3 reveal that the thicknesses of films are ca. 9 and 7 μm, respectively, which are estimated from the depth (μm) in which the signal intensity of the Au substrate is at half-maximum value. The denser and more compact surface of the PPy/clay composite film, as shown in the SEM imagine, may be responsible for a thinner layer obtained. As shown in Figure 3(b), the depth profile of the main element, Si, in clay, the spatial distribution of clay particles in the composite is quite uniform.

The XRD analysis of the very-similar patterns in Figure 4 shows that the incorporation of clay in the PPy film has no apparent influence on the crystallization of its growth and the intercalation of PPy into the clay lamellae is hard observed. The phenomenon of no intercalation was also reported in the chemical preparation of polyaniline/clay nanocomposites.[41] This is reasonable, because in the presence of clay, the electropolymerization of the PPy/clay composite is rapid and the polymer being deposited on the Au substrate is not intercalated, but is simply coated on the surface of the clay particles, as in the inorganic oxide system. A similar feature was shown in the XRD analysis of the poly(*N*-vinylcarbazole) and $FeCl_3$-impregnated clay nanocomposite system.[19]

Figure 5 shows the TGA analyses for pure PPy and the PPy matrix in the PPy/clay composite. Because of the thermal stability of the clay, and in order to allow a better comparison between the analyses of PPy and clay-PPy films, curve b in this figure demonstrates the weight change of the PPy matrix in the PPy/clay

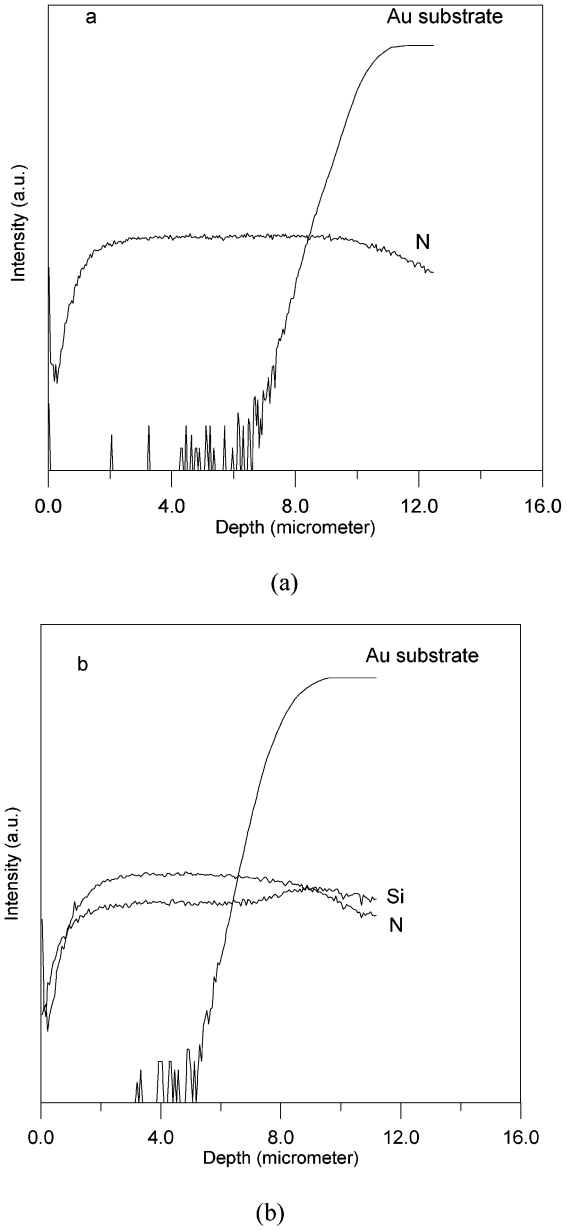

Figure 3. Depth profile of Si in the PPy/clay composite.

composite. This TGA analysis is based on the weight change of the PPy/clay composite and the weight percentage of the PPy matrix in this composite, which can be obtained from a TGA test of the PPy/clay composite to 800 °C in air, in which the residue is just the pure clay. The obtained weight percentage of PPy in the composite is therefore to be 90.5%. As shown in Figure 5, a serious degradation of pure PPy beginning at ca. 200 °C is observed, and the weight loss reaches 73.2% at the ending temperature of 800 °C. Encouragingly, for the PPy/clay composite, the obvious degradation begins at ca. 300 °C and the degradation is depressed at ca. 450 °C. At the ending temperature of 800 °C, the weight loss of the PPy matrix in the PPy/clay composite is just 44.0%. Also, the temperatures at the 10% weight loss for the pure PPy and the PPy/clay composite are 170 and 296 °C, respectively. Clearly, the electropolymerized PPy/clay composite becomes more stable in this study, although Yeh et al.[24] reported that the thermal stability of the chemically synthesized

(41) Kim, B. H.; Jung, J. H.; Kim, J. W.; Choi, H. J.; Joo, J. *Synth. Met.* **2001**, *121*, 1311.
(42) Kim, B. H.; Jung, J. H.; Hong, S. H.; Kim, J. W.; Choi, H. J.; Joo, J. *Curr. Appl. Phys.* **2001**, *1*, 112.
(43) Bhattacharya, A.; Ganguly, K. M.; De, A.; Sarkar, S. *Mater. Res. Bull.* **1996**, *31*, 527.

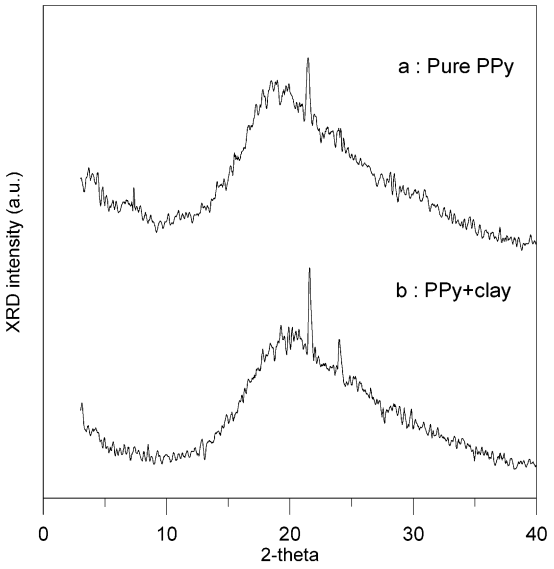

Figure 4. XRD patterns of PPy-based films: (a) unmodified PPy film; (b) PPy film with caprolactam-modified clay.

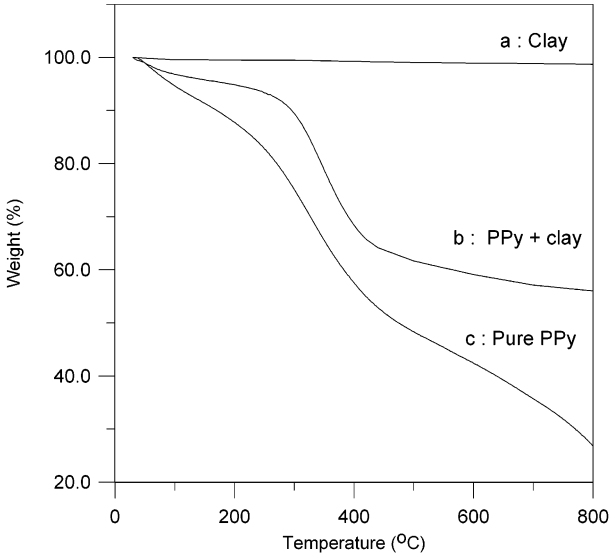

Figure 5. TGA curves of caprolactam-modified clay and different PPy-based films. Experiments were performed in nitrogen. (a) Clay. (b) PPy matrix in the PPy/clay composite. (c) Pure PPy.

polyaniline/clay nanocomposite is not expected to be better than that of unmodified polyaniline.

Figure 6 shows the Raman spectra of pure PPy and the PPy/clay composite films. As shown in the literature,[44,45] the peak located at from 1560 to 1630 cm^{-1} represents the C═C backbone stretching of PPy. This peak position can be used to evaluate the conjugating length of polymer chains, which is closely related to the conductivity of PPy.[46] The results of the peaks positions of the C═C backbone stretching being 1589 and 1603 cm^{-1} for pure PPy and the PPy/clay composite, respectively, indicate that the conjugating length of the latter is shorter than the former, which is contrary to the corresponding performance in conductivity. Hence, it is

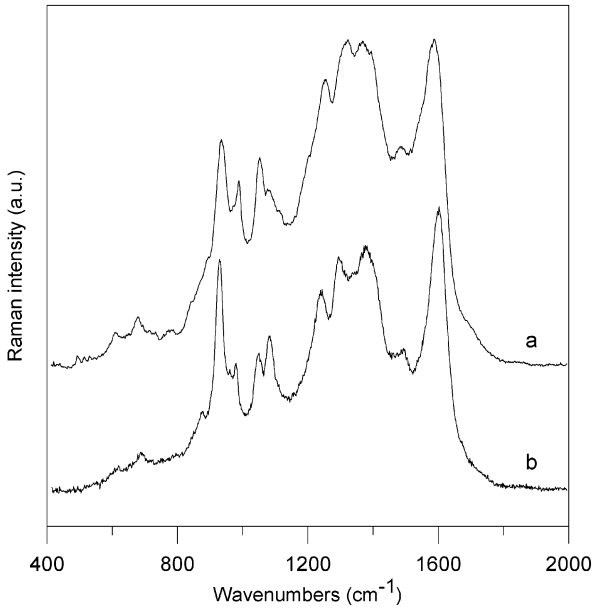

Figure 6. Raman spectra of different PPy-based films. Curves a (upper line) and b (lower line) represent pure PPy and the PPy/clay composite, respectively.

essential to examine other vibrational modes to explain their differences in conductivity. As shown in the previous study,[47] the peak shown at the higher frequency of the double peaks at about 1052 and 1083 cm^{-1} in SERS is assigned to be the C−H in-plane deformation of oxidized PPy. The conductivity of PPy is strongly related to, and increases with, this Raman peak intensity of oxidized PPy. Thus, the broader Raman peaks of PPy appearing in the range of 1000∼1150 cm^{-1} shown in Figure 6 were further deconvoluted into their individual reduced and oxidized component peaks which are located at 1051 and 1080 cm^{-1}, and 1050 and 1082 cm^{-1} for pure PPy and the PPy/clay composite, respectively, as demonstrated in Figure 7. Here we use the oxidation degree (which is defined as the ratio of the area of oxidized PPy to that of total component peaks in this region of C−H in-plane deformation) to quantitatively relate the corresponding conductivity of PPy. The calculated oxidation degrees are 0.41 and 0.59 for pure PPy and the PPy/clay composite, respectively. The higher oxidation degree demonstrates a positive effect on more electron holes available which are favorable for the electron hopping along the polymer chains. This effect of enhancing conductivity significantly exceeds the loss in conductivity due to the shorter conjugating length. Therefore, a higher conductivity of the PPy/clay composite is observed.

Figure 8 shows the XPS N 1s spectra of as-grown and aged PPy-based films. Generally, the XPS N 1s spectrum of PPy is deconvoluted into four component peaks with equal specified value of HWHM to the utmost. One is a larger peak at 399.8 eV, which is assigned to the amine (−NH−) nitrogen. Another is a smaller peak at 398.0 eV, being attributable to the imine (−N═) nitrogen. The others attributed to the positively charged nitrogen ($-N^+H-$) species are shown in the higher binding energy (BE) tail (BE > 401 eV), which can be

(44) Zhong, C. J.; Tang, Z. Q.; Tian, Z. W. *J. Phys. Chem.* **1990**, *94*, 2171.
(45) Schantz, S.; Torell, M. *J. Appl. Phys.* **1988**, *64*, 2038.
(46) Tian, B.; Zerbi, G. *J. Chem. Phys.* **1990**, *92*, 3892.
(47) Liu, Y. C.; Hwang, B. J. *Synth. Met.* **2000**, *113*, 203.

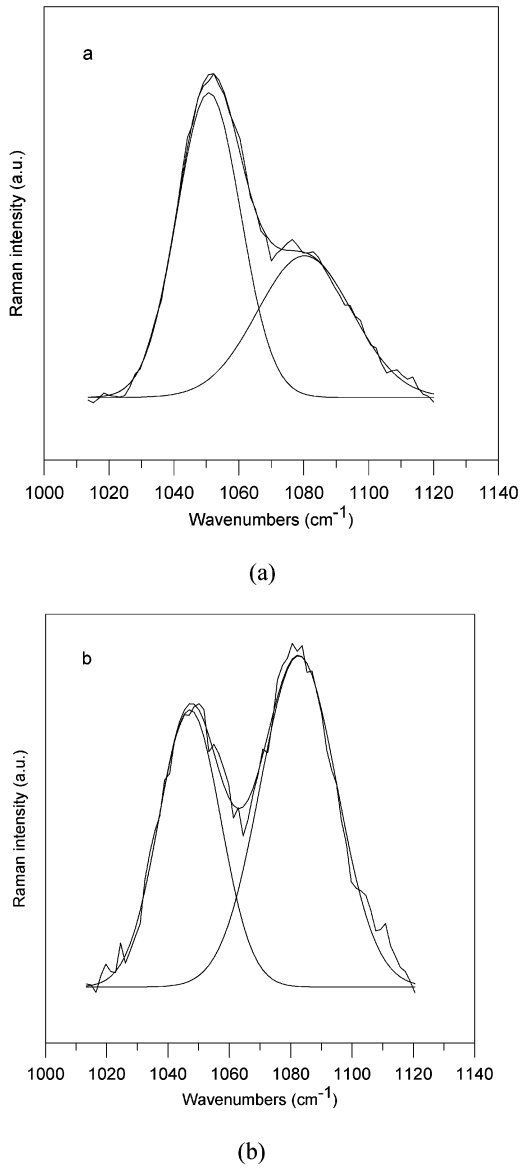

Figure 7. Raman double peaks of C−H in-plane deformation of different PPy-based films: (a) pure PPy; (b) PPy/clay composite.

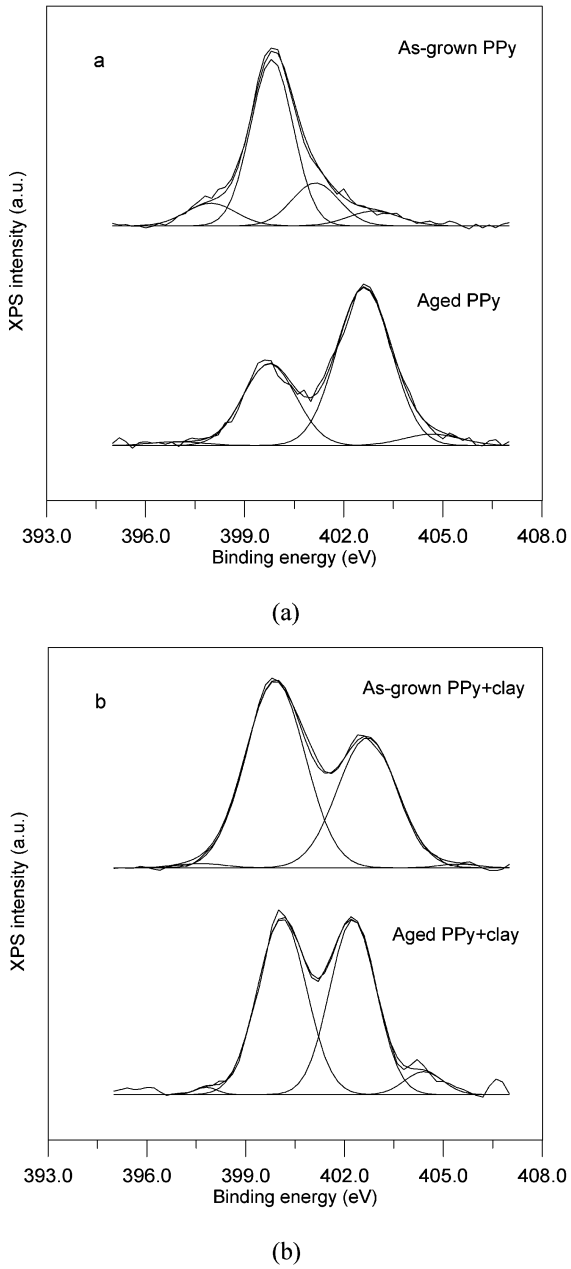

Figure 8. XPS N 1s core-level spectra of as-grown and aged PPy-based films: (a) pure PPy; (b) PPy/clay composite.

used to define the oxidation level of PPy.[48,49] This oxidation level is calculated from the ratio of the peak area of N^+ (BE > 401 eV) to that of the total N 1s shown in the XPS spectrum. The results indicate that the oxidation levels are 0.25 and 0.41 for the as-grown pure PPy and the PPy/clay composite, respectively, which are reasonable for the corresponding conductivities obtained.[50] As shown in Figure 8, the HWHM of the as-grown PPy/clay composite is significantly higher than that of the as-grown pure PPy; which may be ascribed to a special electropolymerization mechanism for pyrrole polymerized with lamellar clay. Generally, the oxidation level of as-grown PPy ranges from 0.25 to 0.33.[50] The resulting unusually high oxidation level of 0.41 for PPy polymerized at lower anodic potential of 0.85 V versus Ag/AgCl in the caprolactam-modified clay-containing electrolyte, as compared with the previous studies,[37,38] is interesting. Higher oxidation level means more available electron holes, which are contributive to electrons hopping along the polymer chains. Thus a correspondingly extremely high conductivity of the PPy/clay composite is obtained.

Aging Test. To evaluate the effect of the incorporation of clay particles into the PPy matrix on the anti-aging ability of the resulting composite, pure PPy and the PPy/clay composite were placed in an atmosphere of 50% RH and 20% (v/v) O_2 at 30 °C for 60 days. The detailed mechanisms of conductivity decay for PPy exposed to oxygen and water atmospheres were proposed in the previous reports.[37,38] After aging, the increase of N^+ species comes from the charge-transfer interactions with oxygen, forming the N−O species.[51−53] The presence of N−O bonds, thus, forms a barrier to electrons hopping along the polymer chains and across

(48) Kang, E. T.; Neoh, K. G.; Ong, Y. K.; Tan, K. L.; Kan, B. T. *Macromolecules* **1991**, *24*, 2822.
(49) Eaves, J. G.; Kopelove, A. B. *Polym. Commun.* **1987**, *28*, 38.
(50) Skotheim, T. A. *Handbook of Conducting Polymers*; Marcel Dekker: New York, 1986; Chapter 8, p 275.

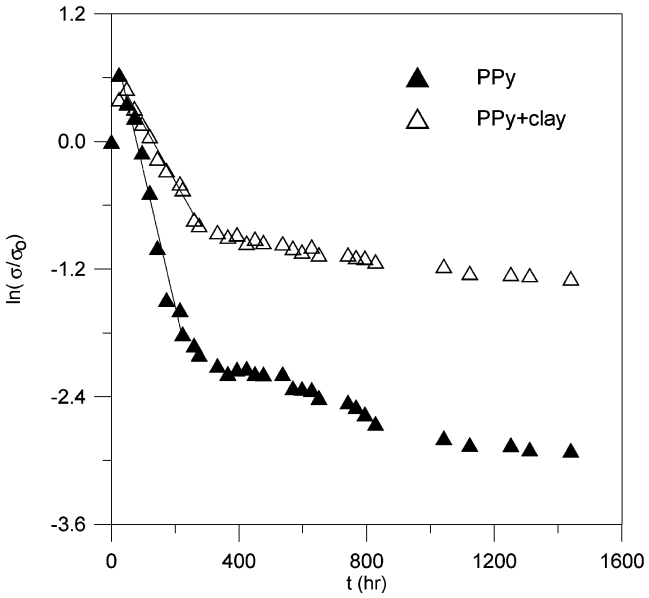

Figure 9. Variation of the electronic conductivity for PPy-based films in 50% RH and 20% (v/v) O_2 at 30 °C for 60 days. Solid and open triangles represent pure PPy and the PPy/clay composite, respectively.

the interchains. As a result, the N^+/N ratio increases, ascribed to the N−O species having a detrimental effect on conductivity. As shown in Figure 8, the N^+/N ratios increase from 0.25 to an extremely high level of 0.67 and from 0.41 to 0.51 for the pure PPy and the PPy/clay composite, respectively, after aging, which are consistent with the corresponding decreases in conductivities from 26.4 to 1.45 S cm^{-1} and from 322 to 89.2 S cm^{-1} for pure PPy and the PPy/clay composite, respectively. This reveals that pure PPy seriously decays, but the modification of clay particles can depress its aging.

Figure 9 demonstrates the conductivity decay as a function of aging time. The phenomenon of the increase in conductivity during the first 24 and 48 h for pure PPy and the PPy/clay composite, respectively, was also reported in the previous study of PPy exposed to an atmosphere of 50% RH.[37] This increase in conductivity during these hours can be ascribed to the solvation of the incorporated salt. The linear slope of conductivity decay plot (excepting the first 24 and 48 h for pure PPy and the PPy/clay composite, respectively) indicates that the process can be fitted to a first-order reaction kinetic in 24 to 240 h and in 48 to 264 h for pure PPy and the PPy/clay composite, respectively, according to

$$\ln(\sigma/\sigma_o) = -kt \qquad (1)$$

where k is the degradation constant, σ and σ_o are the conductivities of PPy-based films at time t in aging and as-grown PPy-based films, respectively. The calculated degradation rate constants are 12.8 and 5.41×10^{-3} hr^{-1} for pure PPy and the PPy/clay composite, respectively. Moreover, after 60 days of testing, the conductivity decreases by 94.5% and by 72.3% for pure PPy and the PPy/clay composite, respectively. Clearly, the electropolymerized PPy/clay composite becomes more stable.

Comparison of Conductivity to Other Works. Nanodimensional composites of CP with MMT-based clay are usually chemically prepared by intercalation. However, some reports revealed that intercalation is disadvantageous to the conductivity of resulting CP/clay nanocomposites because the clay layers may interrupt the effective doping process.[23,41,42] As reported by Cho et al.[26] in the study of PPy-coated nanosized novel ceramics, the high contact conductivity originated from the enhanced molecular order of polymer chains that were grown in the nanoscopically confined environment. All of these results may imply that the clay lamellae provides an environment for the initial growth of ordered PPy films. The subsequent growth of PPy is not intercalated, but is simply coated on the surface of the clay particles resulting in the PPy/clay composite with an enhanced conductivity. To prove this postulate, two other kinds of clays, Na^+-MMT and poly-(vinylpyrrolidone, C_6H_9NO)-modified MMT with interlayer spacings of 7.2 and 24.8 Å, respectively, were also used to prepare the PPy/clay composites. The conductivities of the PPy-based composites with Na^+-MMT, caprolactam-modified MMT, and poly-(vinylpyrrolidone)-modified MMT clays are 634, 322, and 118 S cm^{-1}, respectively, which are inversely proportional to the corresponding interlayer spacings of the clays used. Therefore, higher interlayer spacing of lamellae in clay is advantageous to the intercalation, but is disadvantageous to the conductivity, of the resulting PPy/clay composite.

Conclusion

In this study, a PPy/clay composite was successfully electropolymerized on a gold substrate at 0.85 V versus Ag/AgCl in the caprolactam-modified MMT clay-containing aqueous solution. Basically, before and after nuclei overlapping (i_m), the experimental curves for both pure PPy and the PPy/clay composite are more or less consistent with the theoretical curve of the 3D instantaneous nucleation, but a positive deviation of i/i_m from the theoretical one is observed for the latter. The results indicate that the clay lamellae provide an environment for the initial growth of ordered PPy films. The subsequent growth of PPy is not intercalated, but is simply coated on the surface of the clay particles. The surface morphology of the resulted composite is denser and more compact. The composite demonstrates an extremely high oxidation level and oxidation degree of 0.41 and 0.59 revealed from the analyses of XPS and SERS, respectively, which are favorable for electron hopping along the polymer chains and a correspondingly higher conductivity performance. Meanwhile, the conductivity of the composite was significantly enhanced from 26.4 S cm^{-1} for pure PPy to 322 S cm^{-1}, and it can depress aging in comparison to pure PPy. The thermal stability of PPy is also improved, as shown from TGA, due to the modification of the incorporated clay.

Acknowledgment. We thank the National Science Council of the Republic of China (NSC-90-2214-E-238-001) and Van Nung Institute of Technology for their financial support.

CM020194C

(51) Cheah, K.; Forsyth, M.; Truong, V. T.; Jacques, C. O. *Synth. Met.* **1997**, *84*, 829.
(52) Hepel, M.; Chen, Y. M.; Stephenson, R. *J. Electrochem. Soc.* **1996**, *143*, 498.
(53) Ribo, J. M.; Dicko, A. *Polymer* **1991**, *32*, 728.